Edinburgh 2002/24
December 2002

Top Pair Production Beyond Double-Pole Approximation: pp, $p\bar{p} \to$ 6 Fermions and 0, 1 or 2 Additional Partons

N. Kauer

School of Physics, University of Edinburgh, Edinburgh EH9 3JZ, UK

Abstract

Hadron collider cross sections for $t\bar{t}$ production and di-lepton, single-lepton and all-jet decays with up to 2 additional jets are calculated using complete LO matrix elements with 6-, 7- and 8-particle final states. The fixed-width, complex-mass and overall-factor schemes (FWS, CMS & OFS) are employed and the quality of narrow-width and double-pole approximations (NWA & DPA) is investigated for inclusive production and suppressed backgrounds to new particle searches. NWA and DPA cross sections differ by 1% or less. The inclusion of sub- and non-resonant amplitudes effects a cross section increase of 5–8% at pp supercolliders, but only minor changes at the Tevatron. On-shell $t\bar{t}/Wtb$ backgrounds for the $H \to WW$ decay in weak boson fusion, the hadronic τ decay of a heavy $H^\pm$ and the $\phi \to hh \to \tau\tau b\bar{b}$ radion decay at the LHC are updated, with corrections ranging from 3% to 30%. FWS and CMS cross sections are uniformly consistent, but OFS cross sections are up to 6% smaller for some backgrounds.

I. INTRODUCTION

Since the discovery of the top quark in 1995 [1], the capabilities of ongoing and forthcoming collider experiments have improved significantly. Consequently, $t\bar{t}$ production will be abundant and studied intensely as a signal at Fermilab's Tevatron collider and even more so at CERN's Large Hadron Collider (LHC). With a decay width Γ_t of about 1.5 GeV the top quark decays too rapidly to be observed directly, and is instead identified through characteristic detector signatures with isolated leptons and jets. These signatures would also be observed in the production of various hypothetical particles, so that top production constitutes an important background for many new particle searches. In light of the changed role that top production will play in the near future, the quality of corresponding theoretical predictions needs to be reviewed.

As is well known, a general, systematic and "natural" treatment of unstable particles in perturbative field theory is not straightforward.[1] Signal cross sections that are dominated by the production and decay of unstable particles with $\Gamma/m \ll 1$ can be calculated with good accuracy in narrow-width approximation (NWA). This and similar approximations, like the leading-pole approximation, focus on contributions on or close to resonance and thus greatly simplify calculations, since the production and decay of unstable particles (largely) factorises. They have been widely employed to predict inclusive and exclusive cross sections. Their use to determine background rates for experiments with restrictive selection cuts that eliminate resonant contributions and emphasise peripheral phase space regions can be problematic. In such cases, users of general-purpose event generators like PYTHIA [2] and HERWIG [3] have applied a suggestive procedure that combines results in NWA at the cross section level. For $t\bar{t}$ backgrounds, for example, $t\bar{t}$ and Wtb results are added to account for double- and single-resonant contributions. Since $t\bar{t}$ calculations in NWA implicitly contain sub- and non-resonant contributions that have been integrated out, this procedure can lead to significant double-counting [4]. It also neglects interference effects: top pair production and associated top (Wtb) production are specialisations of one and the same process, since initial and final states of both "processes" are identical. Furthermore, calculations in NWA often do not include full spin correlations.

[1] Even limited, appealing schemes like the fermion-loop scheme become rather involved for all but the simplest applications [5, 6].

Examples of new particle searches at present and future hadron colliders with substantial $t\bar{t}$ and Wtb backgrounds include $H \to W^+W^-$ [7, 8, 9, 10, 11, 12] and $H \to \tau^+\tau^-$ [9, 13, 14] decays, leptonic signals for cascade decays of supersymmetric particles [15], the Randall-Sundrum radion decays $\phi \to W^+W^- \to \ell^+\ell^-\nu\bar{\nu}$ [16] and $\phi \to hh \to b\bar{b}\tau^+\tau^-$ [17], and searches for $H^- \to \tau_L^-\nu$ in models with a singlet neutrino in large extra dimensions [18]. Reliable phenomenological studies of these searches require tools that allow accurate calculations of top pair production and decay in resonant as well as non-resonant phase space regions and that are not susceptible to the shortcomings mentioned above. The calculations should therefore employ complete matrix elements, i.e. the sum of all leading-order (LO) amplitudes. These matrix elements – in fact all resonant fixed-order amplitudes – exhibit unphysical singularities, and a finite-width scheme has to be applied to reflect that in field theory propagators of unstable particles acquire complex poles when self-energies are resummed to all orders. The set of higher-order contributions that has to be included to adequately model finite-width effects is not uniquely determined. Moreover, variations of higher order in Γ/m, as well as exclusion of problematic phase space regions, e.g. thresholds, are permissible. Consequently, a variety of competing schemes exists [5, 6, 19, 20, 21].

The purpose of this paper is to compare leading-order $t\bar{t}$ cross sections calculated in narrow-width or double-pole approximation (DPA) to cross sections that take into account all sub- and non-resonant amplitude contributions, and to investigate the consistency of several practical finite-width schemes. The program we developed for this purpose is described in Section II, with particular emphasis of finite-width schemes and their implementation. In Section III A results for inclusive top pair production are presented, followed by results for important top backgrounds to new particle searches in and beyond the Standard Model (SM) in Sections III B and III C, respectively. In Section IV, we conclude with a summary and outlook.

II. PROGRAM DESCRIPTION

We introduce a LO program for $t\bar{t}$ production at hadron colliders with up to two additional jets that is not specialised to resonant phase space regions and hence has to include complete tree-level matrix elements for the contributing $2 \to 6$, $2 \to 7$ and $2 \to 8$ subprocesses. If the

W^+W^- decay products are abbreviated as $\mathcal{W}$, $t\bar{t}$ production includes the subprocesses

$$gg \to b\bar{b}\,\mathcal{W}\,, \quad q\bar{q} \to b\bar{b}\,\mathcal{W}\,, \tag{1}$$

$t\bar{t}$ + 1 jet production includes the subprocesses

$$gg \to b\bar{b}\,\mathcal{W}\,g\,, \quad q\bar{q} \to b\bar{b}\,\mathcal{W}\,g\,, \quad qg \to b\bar{b}\,\mathcal{W}\,q\,, \quad \bar{q}g \to b\bar{b}\,\mathcal{W}\,\bar{q}\,, \tag{2}$$

and $t\bar{t}$ + 2 jet production includes the subprocesses

$$\begin{aligned} &gg \to b\bar{b}\,\mathcal{W}\,gg\,, \quad q\bar{q} \to b\bar{b}\,\mathcal{W}\,gg\,, \quad qg \to b\bar{b}\,\mathcal{W}\,qg\,, \quad \bar{q}g \to b\bar{b}\,\mathcal{W}\,\bar{q}g\,, \\ &gg \to b\bar{b}\,\mathcal{W}\,q\bar{q}\,, \quad q\bar{q} \to b\bar{b}\,\mathcal{W}\,q\bar{q}\,, \quad qq \to b\bar{b}\,\mathcal{W}\,qq\,, \quad \bar{q}\bar{q} \to b\bar{b}\,\mathcal{W}\,\bar{q}\bar{q}\,. \end{aligned} \tag{3}$$

The program contains subprocess matrix elements for the di-lepton, single-lepton and all-jet decay modes, or more specifically for the following W^+W^- decay final states:

$$\mathcal{W}_{\text{di-lepton}} = \ell^+\nu\;\ell^-\nu\,, \tag{4}$$

$$\mathcal{W}_{\text{single-lepton}} = \ell^+\nu\;q_d\bar{q}_u\,, \tag{5}$$

$$\mathcal{W}_{\text{all-jet}} = q_u\bar{q}_d\;q_d\bar{q}_u\,. \tag{6}$$

For the di-lepton and all-jet decay modes, the program allows to calculate different-flavor samples, e.g. with $\mathcal{W} = e^+\nu_e\;\mu^-\bar{\nu}_\mu$, as well as same-flavor samples, e.g. with $\mathcal{W} = e^+\nu_e\;e^-\bar{\nu}_e$. Additional amplitudes with $(\gamma, Z \to \ell^+\ell^-) \times (Z \to \nu_\ell\bar{\nu}_\ell)$ and $(g, \gamma, Z \to q_u\bar{q}_u) \times (g, \gamma, Z \to q_d\bar{q}_d)$ fragments contribute in the di-lepton and all-jet decay modes, respectively. Moreover, a finite-width scheme has to be chosen when formulating complete LO matrix elements with unstable particles to avoid unphysical singularities in resonant phase space regions that can be removed by including contributions to all orders in perturbation theory.[2] Since no known scheme is satisfactory in every respect, a cross section by cross section comparison of several schemes with complementary properties is suggestive, but requires more than one version of each subprocess matrix element defined above.

Evidently, the creation of all required matrix elements is a considerable task and calls for automation. While the program is generally written in C++ to permit greater code locality and expressiveness, we prefer faster Fortran code for the matrix element evaluation, since its speed determines the program runtime after initial adaptation. Furthermore, to minimize

[2] The Dyson resummation of top quark self-energy contributions is described in Ref. [4].

the matrix element code, the program should use helicity amplitudes in unitary gauge that neglect CKM mixing. MADGRAPH/HELAS [22, 23] is a matrix element generation system that matches our requirements and has recently been extended to processes with 8-10 external particles. Its output is used as starting point for the matrix element code in our program.

MADGRAPH/HELAS matrix elements use the fixed-width scheme (FWS).[3] In the FWS, all propagators of unstable particles are modified according to the following prescription:

$$\frac{1}{p^2 - m^2} \to \frac{1}{p^2 - m^2 + im\Gamma}\,. \tag{7}$$

This substitution is easy to implement, but the resulting matrix elements with Breit-Wigner propagators are not gauge-invariant. As discussed in Refs. [4, 5, 6], calculations that employ gauge-variant amplitudes and receive sizable contributions from sensitive phase space regions can yield highly erroneous results. To remedy this deficiency, various approaches have been suggested in the literature that yield manifestly gauge-invariant matrix elements. The theoretically most appealing approach is arguably the fermion-loop scheme [5, 6]. We do not consider it further here, since it is not applicable to processes with unstable particles that decay into bosons, including $t\bar{t}$ production. Even if it were applicable in the case at hand, it would require as prerequisite an analytic calculation of effective vertices that has not been automatised yet. Its implementation is therefore not straightforward for complex multi-particle processes with several types of unstable particles. For the studies in Section III we therefore implement two practical finite-width schemes that allow automatic matrix element generation for arbitrary processes and guarantee electroweak and $SU(3)$ gauge-invariant results: the complex-mass scheme (CMS) [20] and the overall-factor scheme (OFS) [21].

The CMS introduces Breit-Wigner propagators in a gauge-invariant manner by replacing the masses of all unstable particles with a complex value as follows:

$$m \to \sqrt{m^2 - im\Gamma}\,. \tag{8}$$

This substitution is performed unconditionally and yields, for example, for the top propagator a different expression than the FWS: $i(\not{p} + \sqrt{m_t^2 - im_t\Gamma_t})/(p^2 - m_t^2 + im_t\Gamma_t)$. $\sin^2\theta_W$ and

[3] We use HELAS-3, which implements the fixed-width scheme. Note that the widely-used version 2 of HELAS implements step-width Breit-Wigner propagators, i.e. $1/(p^2 - m^2 + im\Gamma\,\theta(p^2))$. No notable deviations occur in general, since $|p^2 - m^2| \gg m\Gamma$ if $p^2 < 0$ and $\Gamma/m \ll 1$.

dependent quantities also acquire complex values in this scheme, since $\cos\theta_W = m_W/m_Z$. The CMS matrix elements in our program use HELAS-CMS, a modified version of the HELAS library that we created by converting masses and widths from real to complex variables.[4]

The OFS conserves gauge-invariance while introducing Breit-Wigner behaviour by multiplying the complete LO matrix element (with singular propagators for unstable particles) with overall factors:

$$\mathcal{M}_{compl.} \times \frac{p^2 - m^2}{p^2 - m^2 + im\Gamma} = \mathcal{M}_{res.,\text{BW-prop.}} + \mathcal{M}_{non-res.} \times \frac{p^2 - m^2}{p^2 - m^2 + im\Gamma}\,. \tag{9}$$

For each unstable particle type, one factor is applied for every time-like momentum combination that occurs in propagators of that type. The propagators absorb the corresponding factor and transform into Breit-Wigner propagators:

$$\frac{1}{p^2 - m^2} \times \frac{p^2 - m^2}{p^2 - m^2 + im\Gamma} \;\rightarrow\; \frac{1}{p^2 - m^2 + im\Gamma}\,. \tag{10}$$

Amplitudes that are non-resonant with respect to a particular momentum combination do not absorb the corresponding factor, as indicated in Eq. (9). To facilitate the automatic construction of OFS matrix elements a scripting-language program was written that scans MADGRAPH output, and analyses the structure of all contributing amplitudes. Potentially resonant propagators, where one side is only connected to final state particles, are identified and the required overall factors deduced. The script then constructs the overall factor product for each amplitude, and outputs Fortran code that calculates the OFS matrix element. To optimise the code, combinations of overall factors that occur multiple times are evaluated once and the results are reused.

The comparisons presented in Section III also require the calculation of cross sections in double-pole and narrow-width approximation. For that purpose, a second program – in nature similar to the one used to generate OFS matrix elements – eliminates all amplitudes that do not contain potentially resonant t as well as $\bar{t}$ propagators, thus extracting all double-resonant amplitudes with respect to top decay. The generated Fortran code employs the

[4] Complex widths are introduced since MADGRAPH output uses a real constant ZERO for both, vanishing masses and widths, as argument for HELAS calls. In CMS matrix element code we define ZERO as complex parameter and then also have to declare all widths as complex variables to be compatible. Note that all width variables are set to zero in CMS matrix elements, since the widths are contained in the mass variables.

fixed-width scheme and is used in our DPA calculations. The DPA matrix elements are also used in our NWA calculations. To preserve all spin correlations, we choose to implement the NWA directly by calculating with off-shell intermediate top quarks in the $\Gamma_t \to 0$ limit. To that end, the top width is scaled down to $\Gamma_{t,\text{eff}} = \varepsilon\Gamma_t$, and $|\mathcal{M}|^2$ is multiplied by ε^2 to restore the proper normalisation of the total amplitude. For one resonant propagator one has $|\mathcal{M}_{\text{eff}}|^2 = 1/\varepsilon \times |\mathcal{M}|^2$. A setting of $\varepsilon = 1/1000$ is used in the program and yields excellent agreement with NWA implementations with on-shell intermediate top states. In DPA or NWA mode, the program uses a Breit-Wigner mapping for each resonant top propagator that covers a limited range of invariant top quark masses. Neglected contributions from outside this range introduce a non-statistical error. For the background calculations in Sections III B and III C, off-shell top masses were generated in $m_t \pm 65\Gamma_t$ limiting neglected contributions to approximately 1% (see Eq. (19) in Ref. [4]). For the inclusive calculations in Section III A, we increased the range factor to 6500, reducing this error contribution to 0.01%. A comparison of results given in Table I below with results in Table II in Ref. [4] confirms that a range factor of 65 is not sufficient when a total error of less than 1% is desired.

When cross sections for $t\bar{t}$ production with additional jets are calculated with complete matrix elements, one finds that computational complexity increases by a factor of more than 10 for each additional final state particle beyond the $t\bar{t}$ level. Resulting program runtimes quickly exceed what would be considered acceptable for phenomenological studies. To obtain the $t\bar{t}jj$ results presented in Section III B, it was therefore necessary to use state-of-the-art integration techniques and to develop a method to distribute the Monte Carlo sampling over a larger number of processors. The result is OmniComp, a Monte Carlo integration framework based on the adaptive multi-channel techniques introduced in Refs. [24, 25, 26] that allows to conveniently distribute the calculation over many processors in one or more computer clusters.[5] OmniComp further accelerates the computation of hadron collider cross sections through adaptive Monte Carlo summation of subprocess $\otimes$ helicity combination channels. The mapping of sub- and non-resonant phase space regions follows the approach laid out in Ref. [27]. OmniComp and the phase space mapping library are described in more detail in Ref. [28]. A number of tests were applied to verify the correctness of the

[5] We successfully ran programs on up to 16 processors.

program. First, the Lorentz-invariance of the MADGRAPH-generated FWS matrix elements was tested.[6] CMS matrix elements were tested by comparison with corresponding FWS matrix elements after the complex masses and widths in HELAS-CMS had been set to their usual, real values. The automatic generation of OFS matrix elements was tested by comparing with the manually created OFS matrix elements of Ref. [4]. The DPA/NWA matrix elements were verified by comparing NWA cross sections with results from programs with on-shell intermediate top quarks. The phase space and PDF integration has been tested by comparing with known cross sections for the LHC and Tevatron. Moreover, the addition of hadron collider capabilities to the general purpose packages O'Mega & Whizard [29] and AMEGIC++ [30] reached the final stage this year, and a comparison of top production cross sections to cross-check our implementations is planned for the near future.

III. NUMERICAL RESULTS

In this section, we use the program described above to study the difference between cross sections with on-shell (NWA) and off-shell (DPA) intermediate top quarks, to determine the size of corrections when complete LO matrix elements are included, and to search for deviations between results obtained with different finite-width schemes.[7] We first investigate these issues for inclusive top pair production and then turn to suppressed top backgrounds that are important for new particle searches in and beyond the Standard Model.

To cover the energy range of existing and future hadron colliders, cross sections are calculated for the Tevatron ($p\bar{p}$, $\sqrt{s} = 2$ GeV), the LHC (pp, $\sqrt{s} = 14$ TeV) and a Stage-1 VLHC (pp, $\sqrt{s} = 40$ TeV). Unless otherwise noted, all calculations use the following parameters: $m_Z = 91.187$ GeV, $G_F = 1.16637 \times 10^{-5}$ GeV^{-2} and $\alpha(m_Z) = 1/128.92$, which translates at tree-level to $\sin^2\theta_W = 0.23105$ and $m_W = 79.9617$ GeV, as well as the masses $m_t = 175$ GeV, $m_b = 4.4$ GeV and $m_H = 115$ GeV. LO formulas for the decay widths then yield $\Gamma_t = 1.56$ GeV, $\Gamma_W = 2.01$ GeV, $\Gamma_Z = 2.42$ GeV and $\Gamma_H = 0.00323$ GeV. CTEQ6L LO parton distribution functions are employed by default, with $\alpha_s(m_Z) = 0.118$ and the NLO formula. Factorisation and renormalisation scales are fixed at the top mass, except

[6] The Lorentz-invariance of one and the equivalence of two matrix element routines was tested as described in Ref. [4].

[7] Note that all results calculated with our program include full spin correlations (see Section II).

for studies where cross sections with additional jets are taken into account (e.g. in Table III). In this case, the factorisation scale is chosen as $\mu_f = \min(m_T)$ of the top quarks and additional jets. This factorisation scale definition avoids double-counting of contributions that have already been integrated out in the PDFs. The overall strong coupling constant factor is calculated as $(\alpha_s)^n = \Pi_{i=1}^{n} \alpha_s(m_{T,i})$, again using the transverse masses of both top quarks and any additional jets as input. ATLAS detector resolution and b decay effects are modelled as described in Ref. [14], but tagging efficiencies are not taken into account. Monte Carlo integration errors are 0.1% or less for inclusive cross sections and 1% or less for background cross sections.

A. Inclusive Production

For Table I, we choose inclusive $t\bar{t}$ production and decay into the di-lepton final state $b\bar{b}\, e^+\nu_e\, \mu^-\bar{\nu}_\mu$, and compare cross sections in NWA to cross sections with complete matrix elements. First, the size of changes is compared for LHC and Tevatron collisions. Generally one would expect finite-width effects to be of order $\Gamma_t/m_t = 0.009$, and the Tevatron correction is indeed less than 1%. The LHC cross sections, however, is enhanced by a significantly larger factor of 1.06. This effect is not caused by averaged v. exact spin correlations, since our NWA results include full spin correlations. Furthermore, less than 1% of the increase can be attributed to double-resonant off-shell effects (as seen in Table II). The increase is mainly caused by previously omitted sub-resonant contributions. These contributions are also included for the Tevatron. That no sizable increase occurs there can be traced to the fact that the Tevatron cross section is dominated by quark scattering, while the LHC cross section is dominated by gluon scattering. As shown in the two rightmost columns, the large increase is specific to the gluon-initiated process. In fact, the $q\bar{q}$ cross section is slightly reduced when sub- and non-resonant amplitudes are included. A suggestive kinematical interpretation that relates the large increase to off-shell contributions at hard scattering energies below the on-shell top pair production threshold that are amplified by steeply falling PDFs is therefore misleading. A comparison of calculations with CTEQ4L and CTEQ6L shows that recent PDF improvements decrease cross sections uniformly by 18%, thus having little effect on the $\sigma_{\rm FWS}/\sigma_{\rm NWA}$ enhancement factor. For inclusive cross sections, differences between finite-width schemes are expected to be of higher order in Γ_t/m_t. The third com-

TABLE I: Cross sections in NWA and with complete matrix elements for inclusive $t\bar{t}$ production and di-lepton decay ($b\bar{b}\, e^+\nu_e\, \mu^-\bar{\nu}_\mu$). Effects are compared for colliders, PDF sets and finite-width schemes. Tevatron corrections are of order $\Gamma_t/m_t = 0.009$, but LHC corrections are larger. PDF improvements decreased the LHC cross section by 18%, but the correction is robust. FWS, CMS and OFS yield consistent results. All cross sections are given in fb. Note that NWA cross sections include full spin correlations (see Section II).

Collider	$\sigma_{\rm NWA}$	$\sigma_{\rm FWS}$	$\frac{\sigma_{\rm FWS}}{\sigma_{\rm NWA}}$	$\frac{\sigma_{gg,\rm FWS}}{\sigma_{gg,\rm NWA}}$ $(\frac{\sigma_{gg,\rm FWS}}{\sigma_{\rm FWS}})$	$\frac{\sigma_{q\bar{q},\rm FWS}}{\sigma_{q\bar{q},\rm NWA}}$ $(\frac{\sigma_{q\bar{q},\rm FWS}}{\sigma_{\rm FWS}})$
LHC	5.86×10^3	6.19×10^3	1.06	1.06 (88%)	1.00 (12%)
Tevatron	66.5	66.5	1.00	1.10 (5%)	0.99 (95%)

PDF set	$\sigma_{\rm NWA}$	$\sigma_{\rm FWS}$	$\sigma_{\rm FWS}/\sigma_{\rm NWA}$
CTEQ6L	5.86×10^3	6.19×10^3	1.06
CTEQ4L	7.18×10^3	7.58×10^3	1.06

Scheme	σ	$\sigma/\sigma_{\rm NWA}$
NWA	5.86×10^3	1.00
FWS	6.19×10^3	1.06
CMS	6.19×10^3	1.06
OFS	6.18×10^3	1.06

parison in Table I shows that FWS, CMS and OFS yield results that agree when integration errors of 0.1% are taken into account.

Cross section changes when progressing from NWA to DPA and finally to complete LO matrix elements are displayed in Table II for the di-lepton, single-lepton and all-jet channels of inclusive $t\bar{t}$ production at three hadron colliders: Tevatron, LHC, and a Stage-1 VLHC with $\sqrt{s} = 40$ TeV. In all cases the ratios $\sigma_{\rm CMS}/\sigma_{\rm NWA}$ and $\sigma_{\rm CMS}/\sigma_{\rm DPA}$ are very similar: Replacing on-shell with off-shell intermediate top quarks changes cross sections by no more than 1%. Effects are generally small at the Tevatron. At pp supercolliders, on the other hand, cross sections increase uniformly by about 7% for all decay modes and collider energies.

TABLE II: Change of cross sections with complete matrix elements relative to cross sections in NWA for inclusive $t\bar{t}$ production and di-lepton, single-lepton and all-jet decay at the Tevatron, LHC, and Stage-1 VLHC ($\sqrt{s} = 40$ TeV). At pp supercolliders, cross sections increase uniformly by about 7% for all decay modes and collider energies. Effects are similar for cross sections in DPA (shown in parenthesis): replacing on-shell with off-shell intermediate top quarks changes cross sections by 1% or less. The cuts $p_T > 15$ GeV, $|\eta| < 4.5$ and $\Delta R > 0.6$ are applied for channels with singular phase space regions related to massless particles.

	$\sigma_{\rm CMS}/\sigma_{\rm NWA}$ ($\sigma_{\rm CMS}/\sigma_{\rm DPA}$)		
	di-lepton	single-lepton	all-jet
Tevatron	1.00 (1.01)	1.01 (1.02)	1.00 (1.01)
LHC	1.06 (1.06)	1.07 (1.07)	1.07 (1.07)
VLHC	1.06 (1.06)	1.07 (1.06)	1.08 (1.07)

B. Backgrounds to SM Higgs Searches

The unexpectedly large increase of inclusive cross sections at pp supercolliders when sub- and non-resonant contributions are included raises the question how large corresponding effects are for new particle searches with significant $t\bar{t}$ backgrounds. When optimised selection cuts are used to suppress top pair production, the dominant double-resonant $t\bar{t}$ contributions are typically suppressed by factors of order 10^{-4} and the importance of contributions from sub- and non-resonant phase space regions can increase considerably. A central jet veto, e.g.

$$p_{Tj} > 15 \text{ GeV} \quad \text{and} \quad |\eta_j| < 3.2 \,, \tag{11}$$

is very effective in suppressing the $t\bar{t}$ background to inclusive $H \to WW$ searches at the LHC [7, 8, 9, 10]. The veto of Eq. (11) reduces the inclusive cross section of 6 pb to 14 fb when the NWA or DPA is applied, whereas a calculation with complete matrix elements yields 26 fb. Sub- and non-resonant contributions increase the result by a factor 1.8. As in the inclusive case, moving from NWA to DPA or switching finite-width schemes changes the corresponding result very little in comparison. The distributions in Fig. 1 show this relationship for differential cross sections.

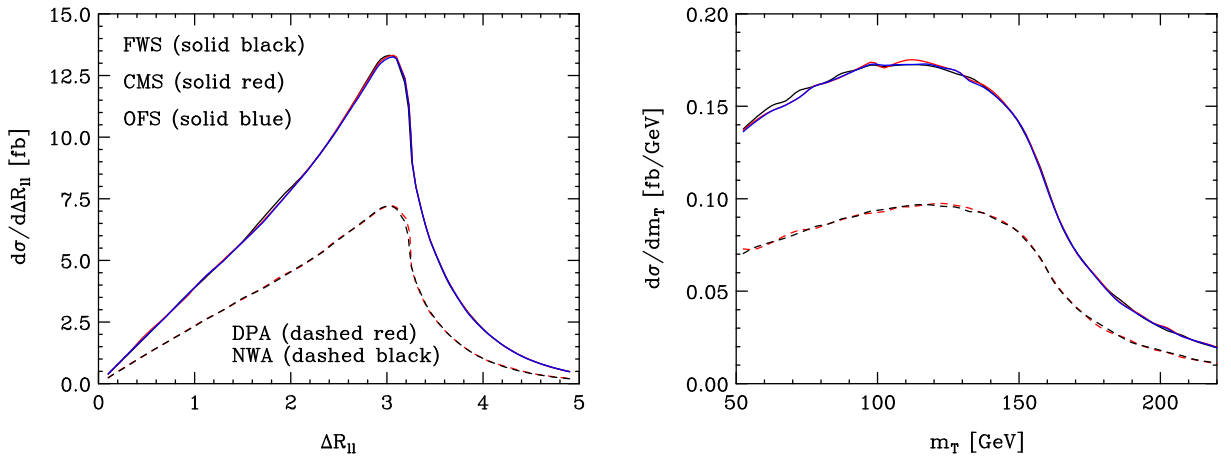

FIG. 1: Charged lepton separation in η-ϕ space and transverse mass distributions for suppressed $t\bar{t}$ production and di-lepton decay ($b\bar{b}\, e^+\nu_e\, \mu^-\bar{\nu}_\mu$) at the LHC. The applied central jet veto ($p_T > 15$ GeV and $|\eta| < 3.2$) reduces the $t\bar{t}$ acceptance to 4×10^{-3}. Differential cross sections with complete matrix elements (solid lines) and in NWA and DPA (dashed lines) are shown. Sub- and non-resonant amplitude contributions enhance the total cross section by a factor 1.8. Off-shell top effects (DPA v. NWA) and deviations between finite-width schemes (FWS, CMS, OFS) are negligible. The transverse mass is defined as $m_T = \sqrt{2p_T^{\ell\ell} \not{E}_T [1 - \cos\Delta\theta(\ell\ell, \not{E}_T)]}$.

TABLE III: Top background cross sections with up to two additional jets for the $H \to WW \to e^\pm\mu^\mp \not{p}_T$ decay search in weak boson fusion at the LHC. The light Higgs-optimised selection cuts and event classification from Ref. [11] are applied. All cross sections are given in fb. Sub- and non-resonant amplitude contributions enhance the total top background by a factor of 1.1. The $t\bar{t}$ background without additional jets is strongly suppressed because in this case both b quarks need to be resolved as forward jets with wide separation in pseudorapidity and very large di-jet invariant mass.

	$t\bar{t}$		$t\bar{t}j$		$t\bar{t}jj$	
	σ	$\sigma/\sigma_{\rm NWA}$	σ	$\sigma/\sigma_{\rm NWA}$	σ	$\sigma/\sigma_{\rm NWA}$
NWA	0.020	1.0	0.94	1.0	0.24	1.0
FWS	0.044	2.1	1.08	1.1	0.24	1.0
CMS	0.044	2.1	1.07	1.1	0.24	1.0
OFS	0.044	2.1	1.07	1.1	0.24	1.0

$H \to WW$ searches are usually tuned for intermediate Higgs masses around 170 GeV, where the $H \to WW$ branching ratio is large. In Ref. [11], the search for $H \to WW$ decays in weak boson fusion at the LHC is studied for the light Higgs ($m_H = 115$ GeV) favoured by LEP experiments [31]. The additional forward jets in weak boson fusion permit powerful selection cut optimisations that make this search channel competitive – a 5σ discovery is possible with 35 fb^{-1} – even for relatively low Higgs masses where the $H \to WW$ branching ratio is small. In this search scenario, $t\bar{t}$ + jets production is the dominant background and its accurate determination is essential. The $t\bar{t}$ background is strongly suppressed, because for final states without additional jets both b quarks need to be resolved as forward jets with wide separation in pseudorapidity and very large di-jet invariant mass. In Ref. [11], complete matrix element corrections were calculated for the $t\bar{t}$ and $t\bar{t}j$ backgrounds using the OFS. As shown in Section III C, OFS cross sections can be artificially reduced. Our program allows to calculate these corrections using the FWS, CMS or OFS. The results are given in Table III and show that the OFS is reliable in this case. Table III also displays first results for $t\bar{t}$+2 jets production calculated with complete LO matrix elements in the literature. Sub- and non-resonant amplitude contributions enhance the total top background by a factor of 1.1.

C. Backgrounds to Beyond-SM Physics Searches

At the LHC, top backgrounds also play an important part in searches for physics beyond the Standard Model. In this section we focus on two studies where $t\bar{t}$ production constitutes the dominant background: the search for hadronic τ decay of a heavy charged Higgs in supersymmetric models and the radion decay $\phi \to hh \to b\bar{b}\tau^+\tau^-$, where one τ decays leptonically and the other hadronically.

The production of a charged Higgs with $m_{H^\pm} > m_t$ in supersymmetric models at high $\tan\beta$ was analysed in Ref. [32]. Production proceeds through $gg \to H^\pm tb$ and is followed by the decays $H^\pm \to \tau\nu$ (with hadronic τ decay) and $t \to jjb$. Applying the selection cuts of this ATLAS study, we calculate $t\bar{t}$ background cross sections in NWA and with complete matrix elements to determine the enhancement factor. The results are shown in Table IV. Sub- and non-resonant amplitude contributions enhance the top background by a factor of 1.1. The ATLAS analysis takes sub-resonant contributions into account by combining $t\bar{t}$ and

TABLE IV: Top background for heavy charged Higgs production $gg \to H^\pm tb$ and decays $H^\pm \to \tau\nu$ (with hadronic τ decay) and $t \to jjb$ at the LHC. The selection cuts of the ATLAS analysis in Ref. [32] are applied. Sub- and non-resonant amplitude contributions enhance the top background by a factor of 1.1. The ATLAS analysis combines $t\bar{t}$ and Wtb results in NWA at the cross-section level. This procedure can lead to substantial double-counting of sub- and non-resonant contributions [4], evidently a 30% effect in the case at hand. All cross sections are given in fb. Parton-level results are rescaled by a factor 0.16, so that our NWA result and the PYTHIA-ATLFAST [2, 33] $t\bar{t}$ result given in Table 3 in Ref. [32] match.

	σ	$\sigma/\sigma_{\rm NWA}$
NWA	0.343	1.00
NWA ($t\bar{t}$ + Wtb)[a]	0.485	1.41
FWS	0.376	1.09
CMS	0.378	1.10
OFS	0.364	1.06

[a]calculated in Ref. [32]

Wtb results in NWA at the cross-section level. This procedure can lead to substantial double-counting of sub- and non-resonant contributions [4]. Our enhancement factor indicates that the actual top background is 23% lower than the estimate in Ref. [32]. In Ref. [18], the analysis was extended to the search for $H^- \to \tau_L^- \nu$ in models with a singlet neutrino in large extra dimensions, and we expect a similarly reduced top background if sub-resonant contributions are included at the amplitude-level.

In Table V, enhancement factors are given for the top background to the decay $\phi \to hh \to b\bar{b}\tau^+\tau^-$ of a Randall-Sundrum radion with mass 300 GeV. The two τ leptons decay leptonically and hadronically, respectively. The selection cuts of the ATLAS analysis in Ref. [17] are applied. Specific model parameters are given in the table caption. The effect of sub- and non-resonant amplitude contributions is small for this top background, in fact smaller than for inclusive $t\bar{t}$ production.

The OFS cross sections in Tables IV and V are several percent lower than the corresponding FWS and CMS cross sections, which agree within the integration error of 1%. To

TABLE V: Top background for the radion decay $\phi \to hh \to b\bar{b}\tau^+\tau^-$ at the LHC, where one τ decays leptonically and the other hadronically. The selection cuts of the ATLAS analysis in Ref. [17] are applied. The radion vacuum expectation value $\Lambda_\phi = 1$ TeV, the radion-SM Higgs mixing parameter $\xi = 0$, the radion mass $m_\phi = 300$ GeV and the lightest Higgs mass $m_h = 125$ GeV. Our results indicate that sub- and non-resonant amplitude contributions change the top background by not more than 3%. All cross sections are given in fb. Parton-level results are rescaled, so that our NWA result and the PYTHIA-ATLFAST [2, 33] $t\bar{t}$ result given in Table 5 in Ref. [17] match.

	σ	$\sigma/\sigma_{\rm NWA}$
NWA	3.27	1.00
FWS	3.36	1.03
CMS	3.34	1.02
OFS	3.17	0.97

understand why the OFS may not be suitable for all $t\bar{t}$ background calculations, we integrate the small phase space region where both top quarks and the intermediate Z boson are close to resonance. More specifically, we require $|m_{Wb} - m_t| < 2\Gamma_t$ and $|m_{WW} - m_Z| < 2\Gamma_Z$. The results are shown in Table VI. The DPA is excellent and contributions from amplitudes with resonant Z propagator are negligible. In the OFS, the dominant double-resonant top amplitudes are artificially suppressed by the overall factor $|(p_Z^2 - m_Z^2)/(p_Z^2 - m_Z^2 + im_Z\Gamma_Z)| \ll 1$. The resulting OFS cross section is consequently much smaller than CMS or FWS cross sections. This example illustrates that cross sections for multi-resonant processes cannot be calculated reliably with the OFS if sizable contributions arise from phase space regions where several amplitudes with different resonance structure compete. Artificially reduced cross sections can even occur for single-resonant processes, given that non-resonant contributions are sizable in phase space regions close to resonance. The authors of Ref. [5], for example, compared OFS and fermion-loop scheme cross sections for radiative W production and found that OFS results are 30% lower close to threshold. Despite some effort[8], we were unable to find a phase space region, where CMS and FWS cross sections for $t\bar{t}$ production

[8] We considered, for example, the selections $m_{Wb} > 500$ GeV, $|\eta_b| > 3.5$ and $\Delta R_{WW} < 1.0$ for collider energies up to 100 PeV.

TABLE VI: Cross sections for $t\bar{t}$ production with di-lepton decay ($b\bar{b}\, e^+\nu_e\, \mu^-\bar{\nu}_\mu$) at the LHC, calculated in DPA and with complete matrix elements using several finite-width schemes. Only the phase space region where $|m_{WW}-m_Z| < 2\Gamma_Z$ and $|m_{Wb}-m_t| < 2\Gamma_t$ is integrated. In this region Z boson *and* top quark propagators are resonant. The DPA is excellent, i.e. resonant $t\bar{t}$ production dominates. The contribution from amplitudes with a resonant Z propagator is negligible. In this phase space region OFS matrix elements are inadequate, since the dominant double-resonant top amplitudes are artificially suppressed by the overall factor $|(p_Z^2 - m_Z^2)/(p_Z^2 - m_Z^2 + im_Z\Gamma_Z)| \ll 1$. The OFS result is 30% smaller than the CMS and FWS results. All results are given in fb.

	σ	$\sigma/\sigma_{\rm DPA}$
DPA	0.0168	1.00
FWS	0.0170	1.01
CMS	0.0170	1.01
OFS	0.0118	0.70

showed significant discrepancies. We therefore conjecture that calculations employing the gauge-variant fixed-width scheme may be used to obtain reliable predictions for the processes considered here. We note that the reliability of the fixed-width scheme has recently also been established for $e^+e^- \to 6$ fermion processes [34].

Our LO calculations do not include log-enhanced higher-order contributions from collinear $g \to b\bar{b}$ configurations for initial state gluons. An improved treatment would include gb scattering matrix elements convoluted with the b quark PDF. Then, a subtraction of the gluon splitting term would also be required to avoid double-counting [35]. However, the additional net contribution to inclusive $t\bar{t}$ production is less than 2% [36] and can safely be neglected in our analysis in Section III A. In the weak boson fusion Higgs search discussed in Section III B, one or both b quarks have no finite transverse momentum threshold, but collinear contributions are small within typical cuts [4]. For central jet veto suppressed top backgrounds, on the other hand, one would expect more pronounced collinear enhancement. The selection cuts for the $t\bar{t}$ background studies in Section III C require that the b quarks are resolved with a transverse momentum of at least 15 GeV. The collinear region is thus avoided.

IV. SUMMARY AND OUTLOOK

We presented cross sections for top quark pair production at hadron colliders with up to two additional jets resulting in 6-, 7- and 8-particle final states calculated with complete tree-level matrix elements. Our program includes di-lepton, single-lepton and all-jet decay modes, and implements three practical finite-width schemes, i.e. the fixed-width, complex-mass and overall-factor schemes, as well as the narrow-width and double-pole approximation for comparison. While our LO calculations are subject to substantial scale uncertainties, the obtained cross section ratios are expected to be robust. For inclusive production, advancing from NWA to DPA by replacing on-shell with off-shell intermediate top quarks, changes cross sections by 1% or less. The inclusion of sub- and non-resonant amplitudes increases NWA or DPA cross sections by 5–8% at the LHC and VLHC, but has little effect on Tevatron cross sections. Top backgrounds to new particle searches are often suppressed by optimised selection cuts that can enhance the importance of sub- and non-resonant contributions considerably. We updated on-shell $t\bar{t}/Wtb$ background estimates for the $H \to WW$ decay in weak boson fusion, the hadronic τ decay of a heavy $H^\pm$ and the $\phi \to hh \to \tau\tau b\bar{b}$ radion decay at the LHC, and found corrections from 3% to 30%. All calculated FWS and CMS cross sections agree within errors. Gauge-violating effects of the FWS appear to be generally negligible for the processes considered here. Our calculations show further that the OFS may yield underestimated cross sections and should be applied with caution in studies with suppressed top backgrounds.

Because of the large scale uncertainties of LO cross sections, precise absolute predictions for top pair production at hadron colliders cannot be achieved with tree-level calculations. The extension of LO to NLO calculations in the framework of the narrow-width and double-pole approximations was first explored in the context of weak gauge boson production [37] and has recently also been carried out for top pair production at hadron colliders [38]. The results in Section III A imply that sub-resonant contributions need to be included in NLO calculations for inclusive $t\bar{t}$ production at pp supercolliders to achieve a theoretical error of $\mathcal{O}(5\%)$. A common method to improve LO predictions for suppressed top backgrounds is to apply a reaction-specific K-factor, i.e. to rescale all LO results by multiplying with $K = \sigma_{incl,\,\mathrm{NLO}}/\sigma_{incl,\,\mathrm{LO}}$. When sub-resonant and non-resonant phase space regions contribute substantially to cross sections, the merit of such procedures has to be tested by comparing

with fully differential NLO calculations that cover resonant and non-resonant phase space regions. The starting point for a complete NLO calculation of top pair production, i.e. a calculation that is not specialised to the double-resonant phase space region, would be the evaluation of the NLO corrections of the complete matrix element for the $b\bar{b}W^+W^-$ final state. The calculation of the real emission corrections is straightforward, since the W bosons are on-shell. However, the evaluation of the virtual corrections of this $2 \to 4$ process involves 1-loop hexagon amplitudes, whose computation is still very challenging [39]. While the $t\bar{t}+$ jets program described in this paper allows to calculate the real emission component of a complete calculation of $pp \to 6$ fermions at NLO in QCD, the evaluation of the virtual corrections for such $2 \to 6$ processes is well beyond present capabilities. NLO predictions for many-particle processes with multiple scales can be further improved by resumming higher-order contributions with large logarithms, such as $\alpha_s \log(m_t^2/p_{Tj}^2)$ in the case at hand.

In addition to precise and accurate calculations for hard scattering subprocesses, a reliable comparison of theoretical predictions and experimental data also requires the proper inclusion of parton showering, hadronisation and detector effects. To standardise the cooperation of parton-level Monte Carlo programs (with full matrix elements) and showering and hadronisation event generators – which in turn produce input for detector simulations – a generic interface has been specified recently in Ref. [40]. In the near future, we plan to implement this interface and to make our complete LO top pair production program available to interested experimental physicists.

Acknowledgments

We thank T. Stelzer for access to a recent version of MADGRAPH and T. Trefzger for helpful information.

---

[1] F. Abe *et al.* [CDF Collaboration], Phys. Rev. Lett. **74**, 2626 (1995); S. Abachi *et al.* [D0 Collaboration], Phys. Rev. Lett. **74**, 2632 (1995).

[2] T. Sjostrand *et al.*, Comput. Phys. Commun. **135**, 238 (2001).

[3] G. Corcella *et al.*, JHEP **01**, 010 (2001); and [hep-ph/0107071].

[4] N. Kauer and D. Zeppenfeld, Phys. Rev. **D65**, 014021 (2002).

[5] U. Baur and D. Zeppenfeld, Phys. Rev. Lett. **75**, 1002 (1995).

[6] E. N. Argyres *et al.*, Phys. Lett. **B358**, 339 (1995); W. Beenakker *et al.*, Nucl. Phys. **B500**, 255 (1997).

[7] M. Dittmar and H. Dreiner, Phys. Rev. **D55**, 167 (1997); and [hep-ph/9703401].

[8] G. L. Bayatian *et al.*, CMS Technical Proposal, report CERN-LHCC-94-38, (1994); R. Kinnunen and D. Denegri, CMS NOTE 1997/057, (1997); R. Kinnunen and A. Nikitenko, CMS TN/97-106, (1997); R. Kinnunen and D. Denegri, CMS NOTE 1999/037, (1999).

[9] ATLAS Collaboration, report CERN-LHCC-99-15, (1999).

[10] K. Jakobs and T. Trefzger, note ATL-PHYS-2000-015, (2000).

[11] N. Kauer, T. Plehn, D. Rainwater, and D. Zeppenfeld, Phys. Lett. **B503**, 113 (2001).

[12] D. Rainwater and D. Zeppenfeld, Phys. Rev. **D60**, 113004 (1999).

[13] D. Rainwater, D. Zeppenfeld, and K. Hagiwara, Phys. Rev. **D59**, 014037 (1999).

[14] T. Plehn, D. Rainwater, and D. Zeppenfeld, Phys. Rev. **D61**, 093005 (2000).

[15] S. Abel *et al.*, SUGRA Working Group Report, (2000) [hep-ph/0003154]; H. Baer, J. K. Mizukoshi, and X. Tata, Phys. Lett. **B488**, 367 (2000); H. Baer, P. G. Mercadante, X. Tata, and Y. Wang, Phys. Rev. **D62**, 095007 (2000); V. Barger and C. Kao, Phys. Rev. **D60**, 115015 (1999); K. T. Matchev and D. M. Pierce, Phys. Rev. **D60**, 075004 (1999); H. Baer *et al.*, Phys. Rev. **D61**, 095007 (2000); W. Beenakker *et al.*, Phys. Rev. Lett. **83**, 3780 (1999); H. E. Haber and G. L. Kane, Phys. Rept. **117**, 75 (1985).

[16] M. Chaichian, A. Datta, K. Huitu, and Z. H. Yu, Phys. Lett. **B524**, 161 (2002).

[17] G. Azuelos *et al.*, note SN-ATLAS-2002-019, (2002).

[18] K. A. Assamagan and A. Deandrea, note ATL-PHYS-2001-019, (2001).

[19] A. Aeppli, F. Cuypers, and G. J. van Oldenborgh, Phys. Lett. **B314**, 413 (1993).

[20] G. Lopez Castro, J. L. Lucio, and J. Pestieau, Mod. Phys. Lett. **A6**, 3679 (1991); A. Denner, S. Dittmaier, M. Roth, and D. Wackeroth, Nucl. Phys. **B560**, 33 (1999).

[21] U. Baur, J. Vermaseren, and D. Zeppenfeld, Nucl. Phys. **B375**, 3 (1992).

[22] T. Stelzer and W. F. Long, Comput. Phys. Commun. **81**, 357 (1994).

[23] H. Murayama, I. Watanabe, and K. Hagiwara, report KEK-91-11, (1992).

[24] G. P. Lepage, J. Comput. Phys. **27**, 192 (1978); G. P. Lepage, preprint CLNS-80/447, (1980).

[25] R. Kleiss and R. Pittau, Comput. Phys. Commun. **83**, 141 (1994).

[26] T. Ohl, Comput. Phys. Commun. **120**, 13 (1999).

[27] N. Kauer, PhD thesis, (2001).

[28] N. Kauer, in preparation.

[29] M. Moretti, T. Ohl, and J. Reuter, *2nd ECFA/DESY Study 1998-2001*, 1981 (2001) [arXiv:hep-ph/0102195]; W. Kilian, *2nd ECFA/DESY Study 1998-2001*, 1924 (2001).

[30] F. Krauss, R. Kuhn, and G. Soff, JHEP **0202**, 044 (2002).

[31] ALEPH, DELPHI, L3, and OPAL Collaborations, LHWG NOTE/2001-03, (2001) [hep-ex/0107029].

[32] K. A. Assamagan and Y. Coadou, note ATL-PHYS-2000-031, (2000).

[33] E. Richter-Wąs, D. Froidevaux, and L. Poggioli, note ATL-PHYS-98-131, (1998).

[34] S. Dittmaier and M. Roth, Nucl. Phys. **B642**, 307 (2002).

[35] A. S. Belyaev, E. E. Boos, and L. V. Dudko, Phys. Rev. **D59**, 075001 (1999); T. M. P. Tait, Phys. Rev. **D61**, 034001 (2000).

[36] A. Belyaev and E. Boos, Phys. Rev. **D63**, 034012 (2001).

[37] A. Denner, S. Dittmaier, M. Roth, and D. Wackeroth, Nucl. Phys. **B587**, 67 (2000), and references therein.

[38] W. Bernreuther, A. Brandenburg, and Z. G. Si, Phys. Lett. **B483**, 99 (2000); W. Bernreuther, A. Brandenburg, Z. G. Si, and P. Uwer, Phys. Lett. **B509**, 53 (2001); W. Bernreuther, A. Brandenburg, Z. G. Si, and P. Uwer, Phys. Rev. Lett. **87**, 242002 (2001).

[39] T. Binoth, G. Heinrich, and N. Kauer, preprint Edinburgh 2002/16 (2002) [arXiv:hep-ph/0210023], and references therein.

[40] E. Boos *et al.*, in proceedings of Workshop *Physics at TeV Colliders*, Les Houches, France, 21 May - 1 June 2001, [arXiv:hep-ph/0109068].